Article

Electron Impact Ionization in Helium Nanodroplets: Controlling Fragmentation by Active Cooling of Molecular Ions

William K. Lewis, Brian E. Applegate, Judit Sztray, Blint Sztray, Tomas Baer, Raymond J. Bemish, and Roger E. Miller

J. Am. Chem. Soc., **2004**, 126 (36), 11283-11292• DOI: 10.1021/ja030653q • Publication Date (Web): 19 August 2004

J|A|C|S
ARTICLES
Published on Web 08/19/2004

Electron Impact Ionization in Helium Nanodroplets: Controlling Fragmentation by Active Cooling of Molecular Ions

William K. Lewis, Brian E. Applegate, Judit Sztáray, Bálint Sztáray, Tomas Baer, Raymond J. Bemish,† and Roger E. Miller*

Contribution from the Department of Chemistry, University of North Carolina, Chapel Hill, North Carolina 27599

Received December 9, 2003; E-mail: remiller@unc.edu.

Abstract: Reported here is a study of the effects of liquid helium cooling on the fragmentation of ions formed by electron impact mass ionization. The molecules of interest are picked up by the helium nanodroplets as they pass through a low pressure oven. Electron impact ionization of a helium atom in the droplet is followed by resonant charge transfer to neighboring helium atoms. When the charge is transferred to the target molecule, the difference in the ionization potentials between helium and the molecule results in the formation of a vibrationally hot ion. In isolation, the hot parent ion would undergo subsequent fragmentation. On the other hand, if the cooling due to the helium is fast enough, the parent ion will be actively cooled before fragmentation occurs. The target molecule used in the present study is triphenylmethanol (TPM), an important species in synthetic chemistry, used to sterically protect hydroxyl groups. Threshold PhotoElectron PhotoIon COincidence (TPEPICO) experiments are also reported for gas-phase TPM to help quantify the ion energetics resulting from the cooling effects of the helium droplets.

Introduction

The success of mass spectrometry as an almost universal tool for the analysis of compounds and mixtures in the gaseous, liquid, and solid phases is related to the wide range of methods that are available for ionizing the species of interest, including traditional electron impact ionization,[1] chemical ionization,[1,2] electrospray ionization,[3,4] Matrix Assisted Laser Desorption Ionization (MALDI)[5] and photoionization.[1,6] Although fragmentation of the newly formed ion can often be used to great advantage, in many cases providing fingerprints used to identify the species of interest, it can also be a problem, particularly in the analysis of complex mixtures.[7,8] Parent ion fragmentation occurs when the internal energy of the ion is sufficient to access the associated fragmentation channels. This energy can arise from the ionization process itself, which may directly populate highly vibrationally excited states of the ion, or may simply be a result of the thermal energy of the neutral, which for large molecules can be several eV. In the latter case, fragmentation can been reduced by simply cooling the neutral molecule (in a free jet expansion, for example) prior to ionization, as demonstrated by Amirav et al.[9] for cholesterol. The limitation of this approach is that it only reduces or eliminates the thermal component of the excess energy, doing nothing to remove the internal energy arising from the ionization process itself. For example, in photoionization the Franck−Condon factors may access highly vibrationally excited states of the ion. Even in chemical ionization there can be vestiges of these effects,[10,11] resulting in vibrational excitation of the ion.

For systems where vibrational excitation of the ion is unavoidable, even when the softest ionization schemes are used, it is interesting to consider ways in which the ion can be actively cooled before fragmentation can occur. For active cooling of the newly formed ion to be effective, the cooling rate must clearly exceed that of fragmentation. It is well-known that fragmentation rates vary dramatically from one ion to another,[12] with the overall trend being that the lifetimes become longer for larger ions.[12,13] This behavior can be understood in terms of the increasing phase space available to the larger ions, which makes it statistically more difficult for the system to channel the necessary energy into the coordinate that leads to fragmentation.[12] This is certainly good news for the present approach, since the motivation is to develop a method that reduces fragmentation by active cooling of the ions, with particular application to larger molecules.

† Chemical R & D, MS 88-156, Pfizer, Eastern Point Road, Groton, CT 06340.

(1) Vestal, M. L. *Chem. Rev.* **2001**, *101*, 361−375.
(2) Munson, B. *Int. J. Mass. Spectrom. Ion. Processes* **2000**, *200*, 243−251.
(3) Gaskell, S. J. *J. Mass. Spectrom.* **1997**, *32*, 677−688.
(4) Dulcks, T.; Juraschek, R. *J. Aerosol Sci.* **1999**, *30*, 927−943.
(5) Stump, M. J.; Fleming, R. C.; Gong, W.; Jaber, A. J.; Jones, J. J.; Surber, C. W.; Wilkins, C. L. *Appl. Spectrosc. Rev.* **2002**, *37*, 275−303.
(6) Butcher, D. J. *Microchem. J.* **1999**, *62*, 354−362.
(7) Rosell-Mele, A.; Carter, J. F.; Maxwell, J. R. *Rapid. Commun. Mass. Spectrom.* **1999**, *13*, 568−573.
(8) Meyer, T.; Kunkel, M.; Frahm, A. W.; Waidelich, D. *J. Am. Soc. Mass Spectrosc.* **2001**, *12*, 911−925.
(9) Amirav, A. *J. Phys. Chem.* **1990**, *94*, 5200−5202.
(10) Kato, S.; deGouw, J. A.; Lin, C. D.; Bierbaum, V. M.; Leone, S. R. *Chem. Phys. Lett.* **1996**, *256*, 305−311.
(11) Kato, S.; de Gouw, J. A.; Lin, C. D.; Bierbaum, V. M. *J. Chem. Phys.* **1996**, *105*, 5455−5466.
(12) Vekey, K. *J. Mass. Spectrom.* **1996**, *31*, 445−463.
(13) McLuckey, S. A.; Stephenson, J. L. *Mass Spectrom. Rev.* **1998**, *17*, 369−407.

The active cooling approach considered here involves embedding the neutral molecules in helium nanodroplets prior to ionization. Helium nanodroplets are well-known to be extremely cold (0.4 K[14]) and to be very efficient heat baths.[15] Cooling of the embedded molecule or ion results when its internal energy is transferred to the liquid, causing helium atoms to evaporate from the droplets. The helium droplets therefore cool both the neutral molecule (prior to ionization) and the newly formed ion. As discussed below, the neutral molecules are introduced into the droplet by passing the latter through a gas pick-up cell[16] (for low volatility compounds this is an oven). Collisions between the droplets and the gas-phase molecules result in the capture, solvation, and cooling of the latter. The doped droplets then enter an electron impact ionizer, forming a helium ion inside the droplet. Resonant charge transfer between helium atoms[17] allows the charge to migrate through the droplet, eventually reaching the neutral molecule. The large difference in the ionization potentials (IPs) of the helium (24.6 eV) and the molecule (8−15 eV) results in significant heating of the internal degrees of freedom of the molecular ion. Here again, we depend on the rapid transfer of this energy to the liquid helium to prevent fragmentation. In most cases the entire droplet is evaporated during the ion-cooling process, leaving a bare molecular ion to be mass selected by a quadrupole. In cases where the cooling rate is faster than that of fragmentation, a cold parent ion will be formed and we would expect the fragmentation channels to be closed.

The helium droplet method has already been used to study fragmentation and ionization of rare-gas clusters formed in the droplets. In particular, Janda and co-workers[17−22] have studied the fragmentation of Ne_n, Ar_n, and Xe_n, from which they conclude that the resonant charge hopping between the helium atoms occurs approximately three times before the He^+ reacts with a neutral helium atom to form He_2^+, releasing 2.35 eV. There is a high probability that the newly formed He_2^+ will be desolvated[21] during the subsequent cooling process, such that further charge transfer to the dopant molecule is unlikely. For large droplets, where the dopant is on average more than three helium atoms distant from the initially ionized atom, the ionization of the molecule is unlikely. Thus, the probability of charge transfer to the molecule is only large for the small droplets, typically less than approximately 1000 atoms.

The first attempt to study the effects of liquid helium on molecular ion fragmentation was reported by Scheidemann et al.[15] on SF_6. Since the SF_6^+ ion is born on the repulsive part of the associated potential surface, fragmentation occurs so quickly that the helium does not have time to significantly cool the system before the SF_5^+ ion is formed.[15,23] However, all further fragmentation is completely suppressed, indicating highly efficient cooling. Although the cooling provided by the helium was not fast enough to stop the fragmentation of the SF_6^+, other systems are more strongly affected. For example, in a similar experiment by Callicoat et al.,[24] it was observed that droplets containing 15 000 helium atoms were able to prevent the fragmentation of $(NO)_2^+$, such that less than 10% of the $(NO)_2^+$ ions fragmented to $NO^+ + NO$. It is therefore reasonable to suspect that the helium cooling will be quite effective for more complex systems, where the fragmentation rates are known to be slower.

It is interesting to note that the heavier rare gases have also been used to cool and study ions. For example, argon has recently been used to cool $O_2^{-\bullet}(H_2O)_n$ clusters.[25] Of particular interest are studies of the effects of argon clusters on the fragmentation of simple organic ions, including methanol,[26] acetone,[27] dimethyl ether,[28] and methyl formate.[29] There again, evaporation of argon actively cools the molecular ions, and in some cases completely suppresses certain fragmentation channels. Since the organic molecules are bound to the surface of the argon cluster, there is effective steric suppression of fragmentation pathways involving rearrangement of the Ar_n-molecular ion cluster. On the other hand, helium droplets are known to solvate organic dopants,[30] which might be expected to give even more efficient cooling. It is also interesting to note that large solidlike argon clusters are less effective in cooling the molecular ions[26] than smaller liquidlike clusters. In contrast, even very large helium droplets (10^6 atoms/droplet) are liquidlike,[31] making them potentially ideal for ion cooling.

In the present study, we examine the effects of helium solvation on the ionization and fragmentation of triphenylmethanol (TPM or trityl alcohol.) TPM is an interesting test case given its importance in the synthesis of a number of important pharmaceuticals, the trityl groups acting to sterically protect hydroxyl sites.[32] Unfortunately, the same structural properties that make TPM a good protecting group make it (and its ether analogues) rather unstable as gas-phase ions. The cleanest mass spectrum yet reported for this system comes from Buchanan,[33] using chemical ionization, where the primary peak in the spectrum was observed at 243 amu, corresponding to the loss of OH from the parent ion.

The fragmentation of TPM^+ formed by electron impact ionization has been studied by two groups, namely McLafferty et al.[34] and Berlin et al.[35] McLafferty et al. examined the skeletal rearrangements that lead to the formation of the biphenyl ion (m/z 154) plus benzaldehyde, or to its closed shell hydrogenated

(14) Brink, D. M.; Stringari, S. *Z. Phys. D: At., Mol. Clusters* **1990**, *15*, 257−263.
(15) Scheidemann, A.; Schilling, B.; Toennies, J. P. *J. Phys. Chem.* **1993**, *97*, 2128−2138.
(16) Lewerenz, M.; Schilling, B.; Toennies, J. P. *J. Chem. Phys.* **1995**, *102*, 8191−8207.
(17) Callicoatt, B. E.; Forde, K.; Ruchti, T.; Jung, L. L.; Janda, K. C.; Halberstadt, N. *J. Chem. Phys.* **1998**, *108*, 9371−9382.
(18) Ruchti, T.; Forde, K.; Callicoatt, B. E.; Ludwigs, H.; Janda, K. C. *J. Chem. Phys.* **1998**, *109*, 10679−10687.
(19) Ovchinnikov, M.; Grigorenko, B. L.; Janda, K. C.; Apkarian, V. A. *J. Chem. Phys.* **1998**, *108*, 9351−9361.
(20) Halberstadt, N.; Janda, K. C. *Chem. Phys. Lett.* **1998**, *282*, 409−412.
(21) Callicoatt, B. E.; Forde, K.; Jung, L. F.; Ruchti, T.; Janda, K. C. *J. Chem. Phys.* **1998**, *109*, 10195−10200.
(22) Ruchti, T.; Callicoatt, B. E.; Janda, K. C. *Phys. Chem. Chem. Phys.* **2000**, *2*, 4075−4080.
(23) Frochtenicht, R.; Henne, U.; Toennies, J. P.; Ding, A.; Fieber-Erdmann, M.; Drewello, T. *J. Chem. Phys.* **1995**, *104*, 2548−2556.
(24) Callicoatt, B. E.; Mar, D. D.; Apkarian, V. A.; Janda, K. C. *J. Chem. Phys.* **1996**, *105*, 7872−7875.
(25) Weber, J. M.; Kelley, J. A.; Nielsen, S. B.; Ayotte, P.; Johnson, M. A. *Science* **2000**, *287*, 2461−2463.
(26) Stace, A. J. *J. Phys. Chem.* **1986**, *91*, 1509−1515.
(27) Stace, A. J. *J. Am. Chem. Soc.* **1985**, *107*, 755−761.
(28) Stace, A. J. *J. Am. Chem. Soc.* **1983**, *106*, 4380−4385.
(29) Bernard, D. M.; Gotts, N. G.; Stace, A. J. *Int. J. Mass. Spectrom. Ion. Proc.* **1990**, *95*, 327−346.
(30) Hess, H.; Larsen, D. S.; Scheidemann, A. A. *Philos. Mag. B* **1999**, *79*, 1437−1444.
(31) Farnik, M.; Henne, U.; Samelin, B.; Toennies, J. P. *Z. Phys. D* **1997**, *40*, 93−98.
(32) Robertson, J. *Protecting Group Chemistry*; Oxford University Press: New York, 2000.
(33) Buchanan, M. V. *Anal. Chem.* **1984**, *56*, 546−549.
(34) McLafferty, F. W.; Van Lear, G. E.; Kornfeld, R. *J. Am. Chem. Soc.* **1968**, *90*, 6240−6241.
(35) Berlin, K. D.; Shupe, R. D. *Org. Mass. Spectrom.* **1969**, *2*, 447−466.

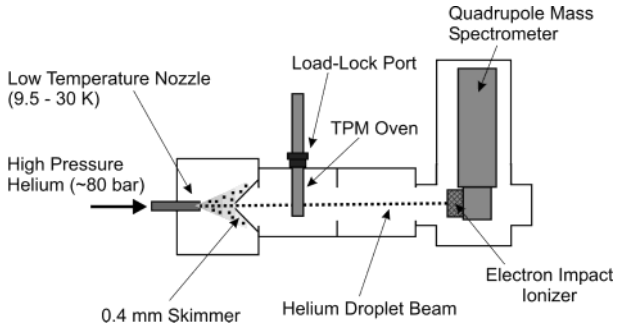

Figure 1. Schematic diagram of the apparatus used in the helium droplet experiments. The droplets are formed by expansion from a high-pressure, low-temperature nozzle. Neutral molecules are absorbed in the oven region. Ionization occurs by electron impact ionization, followed by charge transfer within the droplets, and a mass spectrum is recorded using a quadrupole mass spectrometer.

species, $(Ph)_2H^+$ (*m*/*z* 155), and the C_7H_5O radical. Berlin et al.[35] measured the mass spectra of a series of compounds that produce the trityl ion, $(Ph)_3C^+$, formed from TPM by OH loss.

Threshold photoelectron photoion coincidence (TPEPICO) experiments are also reported here for TPM. These data provide detailed information concerning the dissociation paths and rate constants for this system in the gas phase, which are valuable in the interpretation of the active ion cooling process occurring in the helium nanodroplets experiments.

Experimental Section

Helium Droplet Apparatus. The apparatus used in the present study is shown in Figure 1. The helium droplet source consists of a 5- or 10-μm diameter nozzle, the temperature of which can be varied from 9.5 to 30 K (cooled by a closed cycle helium refrigerator). The expansion of ultrahigh purity helium gas from approximately 80 bar results in the formation of droplets, which pass through a 0.4-mm diameter skimmer, located approximately 20 mm downstream of the source. The source temperature and pressure were varied to produce droplet beams with mean sizes ranging from 5000−40 000 helium atoms. A droplet consisting of 40 000 helium atoms has an evaporation energy of approximately 25 eV, based on the equilibrium value of 5 cm^{-1}/helium atom.[16]

The TPM (Aldrich, 97%) was introduced into the droplets using a heated pickup cell. In most cases, the temperature was adjusted so that the droplets contained, at most, a single TPM molecule. In fact, to avoid contributions from droplets containing more than one molecule, most of the experiments were carried out under conditions where the majority of the droplets were empty, so that the probability of picking up more than one molecule was negligible. Additionally, liquid nitrogen traps were used to cryopump the chamber and reduce droplet contamination. The doped helium droplets were ionized by electron impact ionization and the resulting ions were bent 90° into a quadrupole mass spectrometer (Extrel/Merlin).

It is important to note that the droplet sizes quoted here correspond to the mean of the log-normal distribution,[36] based upon an empirical relationship[37] involving the nozzle temperature, diameter and stagnation pressure. For droplet beam conditions lying outside the region of validity for this empirical relationship, the extrapolations were checked by varying the stagnation pressure and temperature independently, recording the fractional abundance (FA) of the TPM parent ion (defined as the ratio of the parent ion integrated signal to the sum of the integrated signals of all the ions in the mass spectrum). As discussed below, the parent ion FA is quite sensitive to the droplet size, providing us with a method for testing the empirical relationship, by ensuring that different sets of conditions that should gives rise to the same mean droplet size actually do so. From these measurements we conclude that the droplet sizes quoted herein are accurate to approximately 10%.

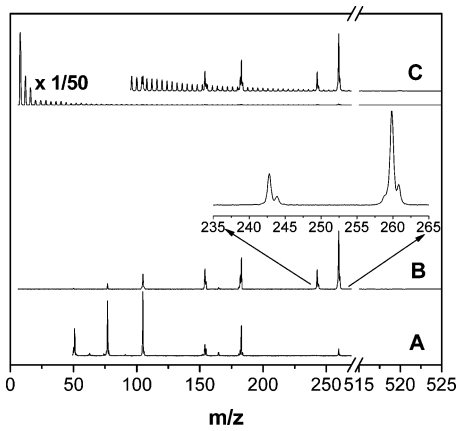

Figure 2. Mass spectra of TPM initiated by electron impact ionization (A) in the gas phase, (B) in helium droplets with the helium ions removed, and (C) in helium droplets showing all the ions.

TPEPICO Apparatus. The threshold photoelectron photoion coincidence (TPEPICO) spectrometer used here has been described in detail previously.[38,39] TPM vapor was introduced into the inlet system by heating the sample to 145 °C. The gaseous sample was photoionized using dispersed, continuous radiation from a hydrogen discharge source. The resulting cations and coincident electrons were extracted in opposite directions by a field of 20 V/cm and the electrons were energy selected by velocity focusing the (initially) zero energy electrons to a 2 mm opening some 12 cm from the ion source.[40] By collecting ions in coincidence with these zero energy electrons, Time-of-flight (TOF) mass spectra were obtained for energy-selected ions by collecting ions in coincidence with these zero-energy electrons, at a series of photon energies. Although the velocity focusing optics used in the present experiment cannot discriminate against electrons that have their velocities directed solely toward the detector, the corresponding effects were removed from the spectra by a procedure detailed by Sztáray and Baer.[41]

The TPEPICO experiments provide fractional abundances for the parent and daughter ions, as a function of the internal energy of the parent ion. In addition, unimolecular dissociation rates can be extracted from the asymmetry of the daughter ion peaks in the TOF spectra, as a function of the ion internal energy. This asymmetry results from the fact that metastable ions dissociate in the first extraction field of the TOF mass spectrometer.

Results

Helium Droplet Mass Spectrometry. In most of the experiments discussed here, the vapor pressure of TPM in the pickup oven was kept as low as possible, to minimize the contributions from droplets containing more than one molecule. Given that the pickup process obeys Poisson statistics,[16] we were able to work under conditions where the probability of picking up more than one molecule was negligible. In fact, the majority of the droplets were empty under these conditions. Figure 2 shows three mass spectra recorded using the helium droplet apparatus.

(36) Lewerenz, M.; Schilling, B.; Toennies, J. P. *Chem. Phys. Lett.* **1993**, *206*, 381−387.
(37) Knuth, E. L.; Schilling, B.; Toennies, J. P. On Scaling Parameters for Predicting Cluster Sizes in Free Jets. In *19th International Symposium on Rarefied Gas Dynamics*; Oxford University Press, 1995; 270−276.
(38) Baer, T.; Booze, J. A.; Weitzel, K. M. *Vacuum Ultraviolet Photoionization and Photodissociation of Molecules and Clusters* **1991**, 259−296.
(39) Keister, J. W.; Baer, T.; Evans, M.; Ng, C. Y.; Hsu, C. W. *J. Phys. Chem. A* **1997**, *101*, 1866−1872.
(40) Baer, T.; Li, Y. *Int. J. Mass. Spectrom. Ion. Processes* **2002**, *219*, 381−389.
(41) Sztáray, B.; Baer, T. *Rev. Sci. Instrum.* **2003**, *74*, 3763−3768.

The spectrum in Figure 2A was recorded with the helium droplet beam turned off and the TPM oven heated to the point where the effusive gas beam emanating from the oven could be detected by the electron impact ionization mass spectrometer. The resulting spectrum agrees quantitatively with the results published in the standard mass spectrum databases.[42]

The spectrum in Figure 2C was obtained with the helium droplet beam turned on and with the oven conditions adjusted to ensure that, at most, one TPM molecule is captured by the droplets, as described above. In fact, the droplet beam was amplitude modulated in this experiment and phase-sensitive detection was used to process the signals. In this way, the background gases in the chamber were not detected. The spectrum shows contributions from both the He_n^+ ion clusters (the peaks spaced by 4 amu) and the TPM that is carried to the ionizer by the droplets. As can be seen in Figure 2C, the He_n^+ ion signals are much more intense than the TPM ion signals, consistent with the fact that only a small fraction of the droplets are doped with TPM. The molecular ion is at 260 amu, while the intensity of the peak at 261 amu is consistent with the natural abundance of ^{13}C. It is important to note that when the helium droplet beam was blocked, all of the TPM peaks disappeared; confirming that the only TPM that contribute to this mass spectrum are those carried by the droplets. Mass spectra were also recorded with the TPM oven at room temperature, so that all of the helium droplets are empty. These were used to remove the He_n^+ peaks from the spectrum in Figure 2C, yielding the mass spectrum in Figure 2B.

The dramatic effect of the helium is immediately apparent from comparing mass spectrum Figure 2B with that of the gas-phase TPM (Figure 2A). Most striking is the fact that the parent ion (260 amu) is strongly enhanced in the Helium Droplet Mass Spectrum (HDMS), in accord with our expectations. Indeed, in the gas-phase MS the parent ion only accounts for 2% of the total ion signal, while in the HDMS the parent ion constitutes approximately 40%. These results already suggest that the cooling rate of the parent ion by the helium is competitive with that of fragmentation for TPM. The qualitative difference between TPM and SF_6 (discussed above) is most likely related to the large difference in the associated fragmentation rates. It is also interesting to note that the 243-amu fragment, which is barely visible in the gas-phase MS, is strongly enhanced in the HDMS, an issue we will discuss further below. The small peak at 244 amu is again consistent with the isotopic abundance of ^{13}C. It must be noted that the present experiment cannot differentiate between a cold molecular ion that is unfragmented and an ion consisting of a neutral fragment that has become weakly associated with its corresponding ionic fragment.[29] The formation of a weakly associated complex, having the same mass as the parent ion, is made possible in the present experiments by the caging effects of the helium. Nevertheless, since we are unable to differentiate between these and the parent ions, for the purposes of the present study we attribute all of the intensity at 260 amu to the molecular ion.

The above data clearly show that the cooling provided by the helium is sufficiently fast to compete with (and thus reduce) fragmentation of the molecular ion. Although we have no direct control over this cooling rate, we can vary the extent of the cooling by changing the droplet size. Large droplets have a correspondingly large evaporation energy (40 000 atoms corresponds to an evaporation energy of approximately 25 eV[16]) and thus the potential for cooling the ions to lower temperatures. In contrast, smaller droplets will completely evaporate before the ion is entirely cooled. Helium droplet mass spectra were recorded over a wide range of droplet source conditions and electron impact energies. Each mass spectrum was analyzed by removing the He_n^+ peaks, as discussed above, and then measuring the integrated areas for the TPM parent and daughter ions. These results were then used to calculate the FA of the parent ion (the parent ion signal divided by the total ion signal). Figure 3 shows the resulting parent ion FAs as a function of the electron impact energy and the mean droplet size (N). We note that the mean droplet sizes have been corrected for the evaporation of helium atoms during the TPM pickup, using the data from Smith[43] to estimate the thermal energy of the TPM molecules. It is immediately clear from Figure 3 that the parent ion FA is highest for the largest droplets, as expected. It is also interesting to note that the parent ion FAs decrease rather abruptly when the electron energy is raised above approximately 50 eV, plateauing again above 80 eV.

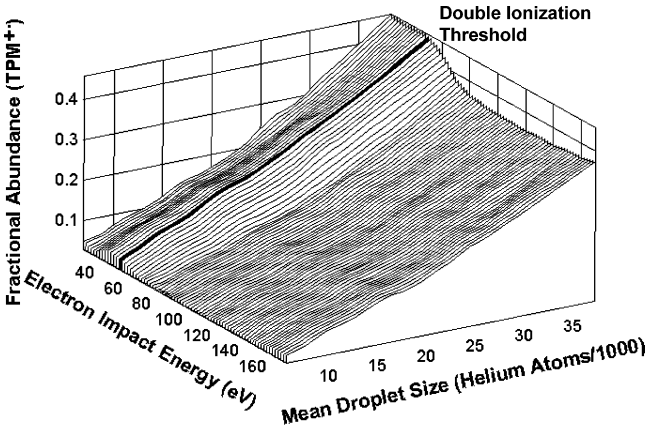

Figure 3. Surface plot of the parent ion fractional abundance (FA) obtained from the HDMS data (for TPM) as a function of the electron impact energy (eV) and the mean droplet size (average amount of helium per droplet).

For comparison, we explicitly note that fragmentation also increases with electron impact ionization in the gas phase. In general, this can be explained by the fact that higher electron energies result in more vibrational excitation of the parent molecular ion. The situation in HDMS is quite different, however, given that the initial ionization step involves ionizing a helium atom in the droplet, and no vibrational excitation of the helium atom is possible. In addition, we expect that the low-frequency modes of the liquid helium will be decoupled from this ionization process. As a result, we must look for a different mechanism for the increased fragmentation that occurs at higher electron impact energies. It is tempting to consider the creation of excited states (2^2S and 2^2P)[44] of the He^+ ion, however the cross sections for producing these states by electron impact are two orders of magnitude smaller than those for the ground-state ions,[45] making their contribution too small to explain the

(42) NIST Mass Spec Data Center, S. E. S. d. "Mass Spectra"; In *NIST Chemistry WebBook, Nist Standard Reference Database Number 69*; Linstrom, P. J., Mallard, W. G., Eds.; National Institute of Standards and Technology: Gaithersburg MD, 2001; http://webbook.nist.gov.

(43) Smith, R. H.; Andrews, D. H. *J. Am. Chem. Soc.* **1931**, *53*, 3644−3660.
(44) Garcia, J. D.; Mack, J. E. *J. Opt. Soc. Am.* **1965**, *55*, 654−685.
(45) Raeker, A.; Bartschat, K.; Reid, R. H. G. *J. Phys. B* **1994**, *27*, 3129−3138.

changes seen in Figure 3. Another possibility is that two He^+ ions are produced in the same droplet, a process that is more likely at higher electron energies. "Coulomb explosion" is familiar from studies of Ar, CO_2, and H_2O clusters[46] and would be expected for doubly ionized helium droplets in the size range used in the present studies, based on the studies of Toennies et al.[31] The subsequent "Coulomb explosion" of the droplets would then reduce the effective droplet size. We observe that the drop in the FAs is not as pronounced for the smaller droplets and lower electron energies, consistent with the correspondingly smaller cross section for creation of a second cation.

There are two possible mechanisms for double ionization: (1) that the two ions are created by two uncorrelated electrons or (2) that they are produced by a single incident electron. Using existing models for droplet ionization,[31] we can estimate that, even for the largest mean droplet sizes and highest electron energies used here, the former accounts for less than 10% of the double ionization events. In addition, the threshold for double ionization via two uncorrelated electrons would be at 24 eV, in contrast with the results in Figure 3, which show a threshold near 50 eV consistent with double ionization from a single electron. Using the Beer's Law approach suggested by Janda,[21] we estimate that a double ionization resulting from a single incident electron occurs in approximately 42% of the largest droplets, again at the highest electron energies.[47] Below 49.2 eV (twice the IP of helium) two He^+ ions cannot be produced, accounting for the higher parent ion FAs (see Figure 3) below 50 eV. The interesting case for the present study is when one He^+ charge transfers to TPM, while the second goes on to form a He_2^+. The latter process will evaporate additional helium from the droplet, reducing the amount available for cooling the TPM ion. Given that charge migration happens much faster than nuclear motion,[20] Coulombic explosion is assumed to occur on the much longer time scale. Clearly, double ionization would be expected to reduce the cooling efficiency and thus give rise to increased fragmentation.

The data set shown in Figure 3 was fitted using a simple model for the above process. The probabilities of forming one or two cations (p_1 and p_2, respectively) for a given mean droplet size and electron impact energy were obtained using the Beer's Law approach[21] mentioned above. The FAs for the parent ion, resulting from single ionization within the droplets (FA_1), were determined from the experimental data obtained below 49 eV, where double ionization from a single incident electron cannot occur. The fractional abundance for doubly ionized droplets (FA_2) was then estimated by noting that the parent ion FAs in Figure 3 increase roughly linearly with mean droplet size. Since the formation of an additional He_2^+ will reduce the effective droplet size, we assume that $FA_2 = (k)(FA_1)$. The experimental data were then fitted using $FA = (p_1)(FA_1) + (p_2)(FA_2)$. The best fit, shown in Figure 4 for the largest mean droplet size, was obtained for $k = 0.57$, suggesting that approximately half of the helium coolant is lost due to the formation of the additional He_2^+. This seems reasonable given that Stace et al.[46] have observed argon clusters that retain 60−65% of their initial mass after a Coulomb explosion. The dashed line in the figure is the expected behavior from two independent electrons, which is clearly inconsistent with the experimental data.

(46) Gotts, N. G.; Lethbridge, P. G.; Stace, A. J. *J. Chem. Phys.* **1992**, *96*, 408−421.
(47) Dogan, M.; Crowe, A. *J. Phys. B* **2000**, *33*, L461−L465.

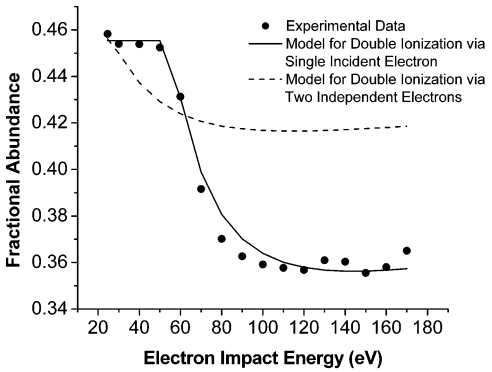

Figure 4. Fractional abundances (FAs) of the parent ion as a function of electron impact energy (eV) and comparison to models for droplet double ionization by one or two incident electron(s).

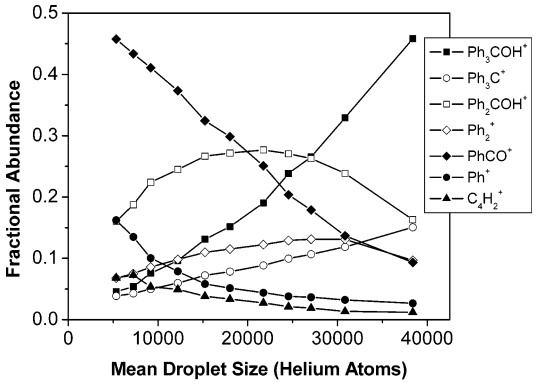

Figure 5. Fractional abundances (FAs) for all of the ions observed in the HDMS as a function of the mean droplet size. The electron impact energy was held constant at 24 eV. The higher generation ions decrease smoothly with increasing droplet size, while the parent ion becomes more intense. First-generation fragments show a nonmonotonic variation with droplet size, as expected.

The results presented above clearly fit our expectations, namely that larger droplets result in more cooling and thus less fragmentation. Unfortunately, we were unable to extend the measurements to even larger droplets (>40 000 atoms) due to the fact that the charge transfer to the TPM becomes improbable for the largest droplets. Indeed, for even larger droplets the only peaks observed in the HDMS are those of He^+_n. As a result, the parent ion FA increases with mean droplet size over the entire range considered here. In the next section we present TPEPICO data that clearly show that the parent ion FA is unity at zero internal energy, the implication being that even for the largest droplet considered here the ions are not completely cooled by the helium. This is despite the fact that at the maximum mean droplet size considered here, namely 40 000 helium atoms, the evaporation energy (25 eV) is more than sufficient to dissipate the energy associated with the IP difference between the molecule and helium. The implication is that the entire evaporation energy of the droplet is not being used to cool the ion, providing us with a clue regarding the nature of the associated processes, as discussed below.

Figure 5 shows the FAs for all of the species observed in the helium droplet mass spectra. As noted above, the parent ion FA increases steadily with increasing mean droplet size, in accordance with our expectations. It is interesting to note that FAs for some of the ions, including Ph^+, $PhCO^+$, and $C_4H_2^+$, decrease monotonically with increasing mean droplet size, while for others, such as Ph_2COH^+ and Ph_2^+, the FAs peak at an

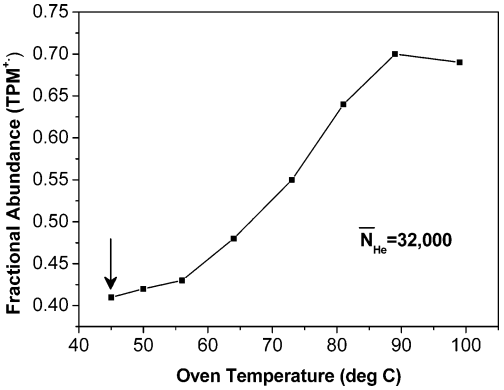

Figure 6. Plot of the parent ion FA as a function of the oven temperature, showing that the fragmentation is greatly reduced when clusters are formed in the droplets. The vertical arrow in the figure shows the conditions used for all of the experiments on the TPM monomer fragmentation.

intermediate mean droplet size. Data of this type clearly differentiate between first and second generation ions, in much the same way as in a TPEPICO experiment (see next section). The results in Figure 5 show that the helium cooling eliminates the second-generation fragments first and then eliminates the primary fragments, consistent with the relative energies of the associated channels.

In an attempt to further reduce the fragmentation in a droplet size range that is accessible to study, we examined the effect of forming clusters of TPM in the droplets by simply increasing the vapor pressure in the TPM oven. Figure 6 shows the results obtained at a fixed average droplet size of 32 000 and the electron impact energy of 24 eV, where the FA of the parent ion was measured as a function of the temperature of the TPM oven, ranging from 45 to 100 °C. Although the TPM vapor pressure is not well determined in this experiment, the mass spectra clearly show evidence for the formation of clusters at the higher oven temperatures. The vertical arrow in the figure shows the conditions used to record all of the data discussed above, where at most a single TPM molecule is present in a given droplet. The parent ion FA clearly increases dramatically when clusters of TPM are formed in the droplets. Although clusters are generally considered undesirable in most mass spectrometer applications, this dependence does suggest that clustering can provide further cooling of the molecular ion. In addition to the increased density of states available to accommodate the excess energy, the ionization of clusters opens up new mechanisms for forming cold ions. For example, although the charge transfer from the helium to one of the TPM molecules in a cluster will first generate a hot ion, the charge could then transfer to a neighboring TPM molecule, leaving the vibrational excitation behind on the original molecule and resulting in the formation of a cold ion.

Another approach for achieving "softer" ionization of the molecule is to coat it with a shell of a heavier rare gas. Since these have lower ionization potentials than helium (Ne = 21.6 eV, Ar = 15.8 eV, and Kr = 14.0 eV), the final charge-transfer step to the molecule will be more gentle. In previous studies[48] we showed that when the rare gas is added to the droplet after the molecule, the tendency is toward the formation of clusters with the molecule embedded in the rare gas.[48] In the limit of complete solvation, the charge transfer will first occur from the

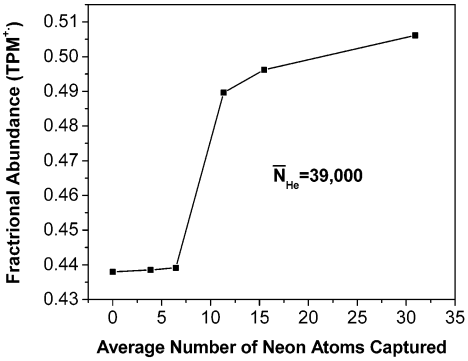

Figure 7. Plot of the parent ion FA as a function of the average number of neon atoms added to the droplets, downstream of the TPM oven.

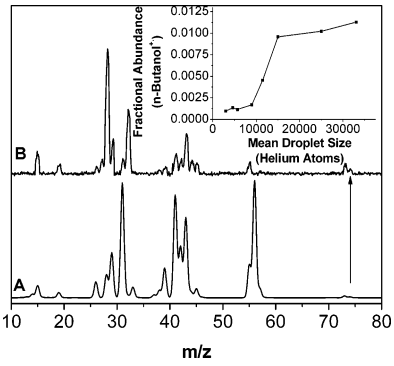

Figure 8. Mass spectra of *n*-butanol in the gas-phase (A) and in the helium droplets (B). The inset shows the parent ion FA as a function of the mean droplet size. The gas-phase mass spectrum was generated from the NIST database and broadened to match the resolution of the present experiments. The arrow denotes the position of the parent ion, $CH_3(CH_2)_3OH^{+\bullet}$.

helium cation to the rare gas shell and then to the molecule. It is interesting to note that previous studies indicate[17,18] that charge transfer from helium to neon results in the emission of a photon from an excited Ne^+ ion, providing a means for removing energy from the system that might otherwise cause fragmentation of the molecular ion.

Figure 7 shows a plot of the parent ion FA as a function of the average number of neon atoms added to droplets consisting of approximately 39 000 helium atoms. Although the magnitude of the effect is quite small, only increasing the FA of the parent ion from 0.438 to 0.51, the dependence on the number of neon atoms is quite interesting. Indeed, there is no effect until the mean number of neon atoms is approximately 10, consistent with the molecule having to be effectively solvated by the neon atoms before the effects of the intermediate charge transfer become significant. The results again plateau above about 20 neon atoms, consistent with the filling of the first solvent shell. It is also interesting to note that neon does not have any effect on the parent ion FA when multiple TPM molecules are present in the droplets, presumably because cluster formation already reduces the fragmentation to a very low level.

To avoid leaving the impression that HDMS is a completely general method for quenching ion fragmentation, we present here a counter-example, namely 1-butanol. We chose this system because the barrier to H_2O loss is very low (0.19 eV) and fragmentation is fast.[49] Figure 8 shows a comparison between an HDMS and a gas-phase mass spectrum, the former corre-

(48) Nauta, K.; Miller, R. E. *J. Chem. Phys.* **2001**, *115*, 10138−10145.

(49) Shao, J. D.; Baer, T.; Lewis, D. K. *J. Phys. Chem.* **1988**, *92*, 5123−5128.

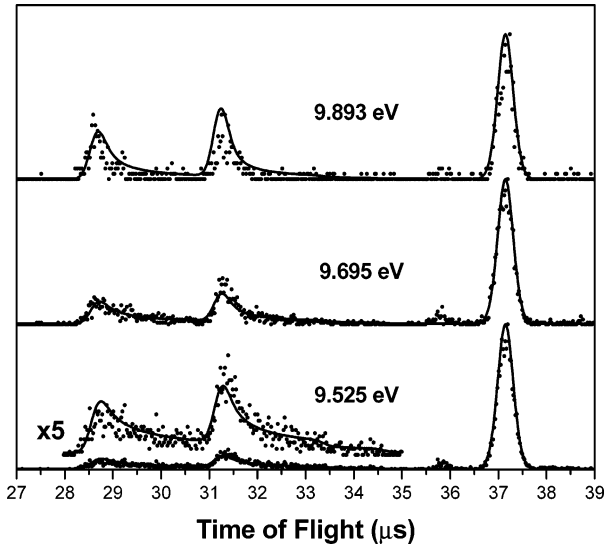

Figure 9. TPEPICO ion TOF distributions obtained at selected photon energies. The points represent the experimental data, while the solid lines show the calculated TOF distributions, based on the methods described in the text. The asymmetric peaks at 31.4 μs and 28.7 μs are assigned to the $(Ph)_2COH^+$ and $(Ph)_2^+$ ions, respectively. The symmetric peak at 37.2 μs belongs to the parent ion, $(Ph)_3COH^+$. Asymmetric peak shapes are a result of slow dissociation.

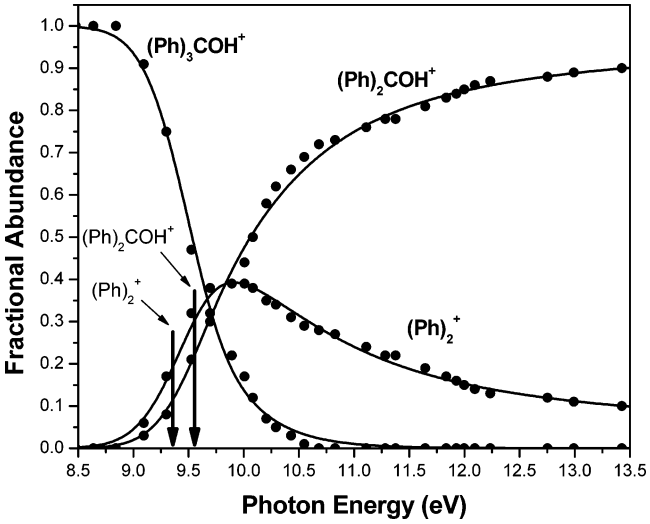

Figure 10. Breakdown diagram for TPM, obtained from the TPEPICO experiments. The experimental data points are fit to the RRKM simulation described in the text, which is represented by the solid lines. The vertical arrows indicate the 0-K appearance energies of the two fragmentation channels.

sponding to the large droplet limit. Although we do see a significant increase in the parent ion FA, in comparison to the gas-phase results, the parent ion FA remains relatively low for all droplet sizes, as shown in the inset. Indeed, the parent ion FA increases from $< 1 \times 10^{-4}$ in the gas phase to approximately 0.01 in helium. It is also interesting to note that the fragmentation pattern is quite different for the two cases.

A quantitative understanding of the results presented in this section requires a more complete understanding of the relative energetics and rates associated with the various fragmentation channels. In the next section we report TPEPICO experiments on TPM that provide such information for gas-phase molecules. Comparisons between the TPEPICO data and the results of the helium droplet experiments provide us with new insights into the effects of the helium on ion fragmentation.

TPEPICO Experiments. The ions in the TPEPICO experiment are collected in coincidence with zero-energy electrons. Thus, the ion internal energy is given by $E_{ion} = h\nu - IE + E_{th}$, where $h\nu$ is the photon energy, IE is the adiabatic ionization energy, and E_{th} is the thermal energy of the molecules at the temperature of the ionization source (ca. 145 °C). The thermal energy is transported to the ion manifold and thus adds to the photon energy. The distribution of internal energy for a molecule such as TPM at 145 °C is quite large, peaking at 0.5 eV and extending well over 1 eV. The ion energy selection is thus severely limited by this thermal distribution of internal energies.

The ionization energy of TPM was determined to be 8.45 ± 0.05 eV by measuring the total ion signal as a function of the photon energy. The ion time-of-flight distributions were then collected at various photon energies, from threshold up to 13.5 eV, the limit of our hydrogen discharge light source. Figure 9 shows several TOF distributions at low energies, near the dissociation onset. Each spectrum required several hours of collection time because of the low TPM vapor pressure. The large peak at 37.0 μs is due to the parent ion, $(Ph)_3COH^+$, with a mass of 260 amu. The two fragment peaks at 28.7 and 31.25 μs are ascribed to $(Ph)_2^+$ and $(Ph)_2COH^+$. The asymmetry of the fragment ion peaks is a result of dissociation in the first 5-cm-long acceleration region. The dissociation rate constant can be determined by modeling these asymmetric TOF distributions, and the solid lines are a result of these calculations. The fact that the rate constant increases with ion energy is evident from the fact that the TOF peaks become correspondingly more symmetric. A very small peak at 35.8 μs has about the correct TOF to be the OH loss product. However, this peak appeared in the spectra at all energies, well below where the major products appeared. Thus, we assign this to an impurity, probably Ph_3CH in the sample.

By recording TOF mass spectra for a range of photon energies, we are able to construct a breakdown diagram (see Figure 10), which is a plot of the fractional abundance of each ion versus photon energy. The two major product ions, Ph_2COH^+ and Ph_2^+, appear at low energy and remain the major ions up to 13.5 eV. The lowest energy fragmentation involves a rearrangement to Ph_2^+ + PhCHO (benzaldehyde). However, the direct dissociation involving phenyl loss quickly takes over and becomes the dominant dissociation product at high energies. Traces of secondary ion dissociation, $Ph_2COH^+ \rightarrow PhCO^+$ and $Ph_2COH^+ \rightarrow Ph^+$, are seen above 12 eV. The first fragment clearly comes from the sequential dissociation of $Ph_2COH^+ \rightarrow PhCO^+ + Ph$. However, the phenyl ion signal could come from either the Ph_2^+ or the Ph_2COH^+ ions. Because the biphenyl ion has a very strong C−C bond energy and is not expected to dissociate easily, and the Ph^+ + PhCHO (benzaldehyde) are quite stable products, we favor the mechanism in which both secondary product ions come from the Ph_2COH^+ ion. However, because these fragment intensities did not exceed 10% and 5%, respectively, their intensities were summed to the corresponding first-generation fragment ion in the breakdown diagram.

The extraction of accurate 0 K dissociation barriers from the above data requires a detailed analysis of the asymmetric TOF distributions, which provide absolute rate constants, and the breakdown diagram, which provides relative rate constants up to 13 eV. The rate constants near the dissociation limit are so slow that the ions cannot dissociate during their 37-μs flight to

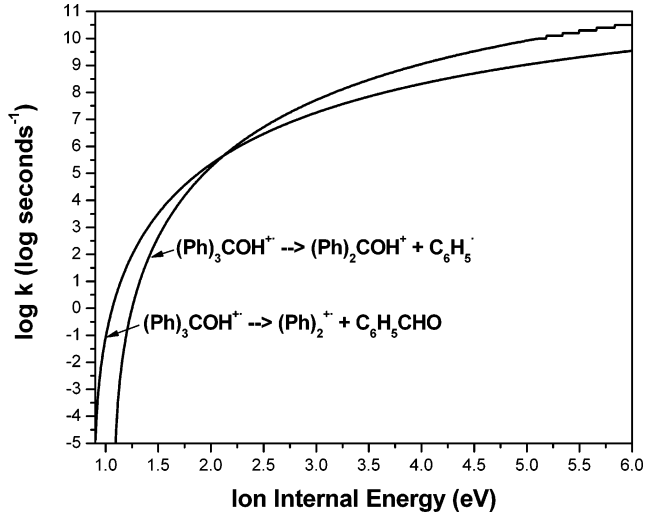

Figure 11. Calculated RRKM rate constants for the two fragmentation channels indicated, based upon the fits to the breakdown curves shown in Figure 10.

the ion detector. Thus, the observed fragmentation onsets are shifted to higher energies, while at the same time the large ion thermal energy lowers the observed onset. The TOF data in Figure 9 and the breakdown diagram in Figure 10 were modeled with calculated rate constants (RRKM theory), including the averaging over the thermal energy distribution, by methods outlined in previous studies.[50,51] The solid lines in these two figures are the result of this analysis, from which we derive the rate constants shown in Figure 11. The only adjustable parameters in fitting these data were the onset energies for the two fragmentation channels and the transition state vibrational frequencies for the two reactions. The molecular ion frequencies were obtained from quantum mechanical calculations using DFT and/or MP2 levels (UHF/RHF 6−311g**) of theory available in the Gaussian 98 suite of programs.[52] The derived 0-K onsets of 9.35 and 9.53 eV are shown as vertical arrows in Figure 10. The 0-K onset is the energy difference between the ground state of the molecule and the ground state of the ionic dissociation products.

Although the rate constants in Figure 11 were calculated with statistical RRKM rate theory, they were fitted to the experiment in two ways. They match the absolute rate measurements in the range from 10^4 to 10^6 sec^{-1}, while at higher energies they are constrained by the relative experimental rate constants of the two dissociation channels, which are determined from the breakdown diagram in Figure 10. The uncertainty in the rate constants is thus quite low in the ion internal energy range from 1.7 to 2.3 eV, but increases with energy, to the point where the expected uncertainty at 5 eV is approximately an order of magnitude. The RRKM rate constants show that at their reaction thresholds, the calculated rate constants are 10^{-5} sec^{-1}, which means that these ions have lifetimes of 10^5 seconds. The ion lifetime of 10 μs, our measurable range, is not attained until the ion internal energy reaches about 1.9 eV.

Discussion

With quantitative information about the gas-phase energetics and fragmentation rates in hand for TPM, we are in a position to make a more detailed examination of the ion cooling in this system. We can begin by using the fragmentation rates determined from the TPEPICO experiments, shown in Figure 11, to obtain an estimate of the cooling rates in helium. From Figure 11 we can estimate that the fragmentation rates in the high-energy regime plateau at approximately 10^{11} sec^{-1}, suggesting that the helium cooling rate must be of comparable magnitude. If we assume the entire 16.1 eV arising from the difference in IPs between helium and TPM is dissipated to the droplet, we obtain a cooling rate of approximately 2×10^{16} K/s. Since there is an uncertainty in the TPEPICO fragmentation rates at high energies of approximately one order of magnitude, our estimate of the cooling rate may also be in error by a similar factor. The present estimate of the cooling rate is consistent with an early study based upon SF_6^+ fragmentation,[15] which yielded 10^{16} K/s. Nevertheless, this agreement could be fortuitous given that a later paper[23] cast some doubt on the validity of the earlier study. In any case, the cooling rate for an ion is likely to be somewhat system dependent.

The data presented in Figure 5 are the helium droplet analogue of a breakdown diagram, with the energy scale being inversely related to the droplet size, and can be compared with the breakdown diagram from the TPEPICO experiments, shown in Figure 10. In the TPEPICO experiment, the dominant products are Ph_2^+ + PhCHO and Ph_2COH^+ + Ph_2, namely the same fragment ions observed in standard electron impact mass spectra.[34,35] Even though the $PhCO^+$ and Ph^+ ions are observed in the TPEPICO experiments, they were summed here into the corresponding first-generation fragment ion signals in the breakdown diagram. In contrast, the HDMS results show a significant FA for the OH loss channel, resulting in the product ion Ph_3C^+. The HDMS results also show some FA for $C_4H_2^+$. The $C_4H_2^+$ may result simply because the energies initially available in the HDMS are larger than those in the TPEPICO experiment, facilitating $Ph^+ \rightarrow C_4H_2^+$. The OH loss channel, which leads to the production of $(Ph)_3C^+$, is extremely weak in the gas-phase electron impact mass spectrum (see Figure 2), suggesting that the helium solvent is doing something more than simply modifying the energetics. One explanation for the relative lack of Ph_3C^+ in the gas phase is that it goes on to form Ph_2^+. This explanation seems unlikely, however, given the high stability of the tertiary carbocations. The TPEPICO data suggest that (in the gas phase) the rates for formation of Ph_2^+ and Ph_2COH^+ are much higher than for Ph_3C^+, particularly at higher photon energies (higher ion internal energies). If the helium were doing nothing more than providing efficient cooling, we would expect that the fragmentation to Ph_2^+ and Ph_2COH^+ would still dominate and there would also be very little Ph_3C^+ in the HDMS experiment.

Since this is not the case (Ph_3C^+ is strongly enhanced in the HDMS), it is possible that the solvation effects of the helium significantly modify the fragmentation pathways. For example, if the helium solvation energy depends significantly upon the identity of the ion, such that the gas phase energetics are not simply shifted by a constant amount, the rates (and hence the branching ratios) could be quite different in helium. Indeed, preliminary ab initio calculations carried out as part of this study indicate that the charge distributions are indeed quite different for the various ions in question, which could result in signifi-

(50) Sztáray, B.; Baer, T. *J. Am. Chem. Soc.* **2000**, *122*, 9219−9226.
(51) Li, Y.; Sztáray, B.; Baer, T. *J. Am. Chem. Soc.* **2001**, *123*, 9388−9396.
(52) Frisch, M. J., et al. Gaussian 98; Gaussian Inc. Pittsburgh, PA, 1998.

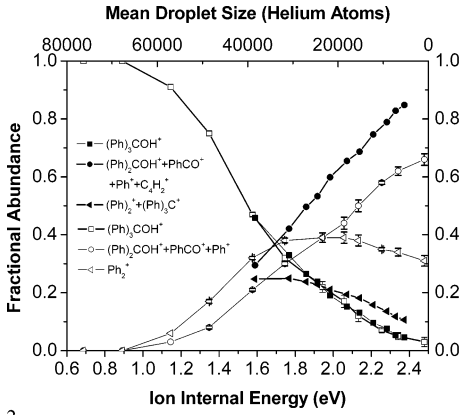

Figure 12. Comparison between the scaled helium nanodroplet data (24 eV electron impact energy) and that obtained from the TPEPICO experiments.

cantly differential solvation. Further experimental and theoretical work will be needed to test this idea.

We now attempt to make a more quantitative comparison between the HDMS results and those of the TPEPICO experiments, the goal being to scale the droplet sizes so that they correspond to the ion energies determined from the TPEPICO experiments. This is best done by comparing the breakdown diagrams from the two experiments, remembering that, in the TPEPICO breakdown diagram, we have summed the first-generation ions with their daughter ions, namely $(Ph)_2COH^+ + PhCO^+ + Ph^+$. Applying the same strategy to the HDMS data, assuming that the $C_4H_2^+$ ion comes from the dissociation of Ph^+ and that the $(Ph)_3C^+$ ion is involved in the lineage of $(Ph)_2^+$, we sum $(Ph)_2COH^+ + PhCO^+ + Ph^+ + C_4H_2^+$ and $(Ph)_3C^+ + (Ph)_2^+$. Figure 12 shows the results from the two experiments, the solid symbols representing the HDMS data and the open symbols the TPEPICO results. The helium droplet size scale has been adjusted to give the best agreement between the two sets of data. It is interesting to note that the qualitative trends are the same in both data sets, with the three FA curves merging at a single ion energy (for the TPEPICO case) or mean droplet size (for the HDMS data). It is the similarity in the curves for the two sets of data that allows us to determine a reasonable scaling between the variables in the two data sets, namely the ion energy and mean droplet size.

Although the agreement between the two data sets is reasonable, (based upon the scaling discussed above) we note that there are a number of factors that make us cautious about the interpretation of these results. First, the ion internal energy distributions are quite different in the two experiments. In the TPEPICO case the data correspond to an average over the thermal distribution at 418 K, while the distribution for the HDMS data is less well defined, but is somehow related to the log-normal distribution of droplet sizes. Second, we already know that the effect of the helium solvent on the fragmentation processes is significant, resulting in different fragmentation channels from those observed in the gas phase. Despite these qualifications, it is interesting to consider the implications of the breakdown diagrams shown in Figure 12, taken at face value.

The scale factor that provides the best overlay of the two breakdown diagrams leads us to some interesting ideas. First we note that extrapolation of the HDMS data to zero droplet size yields a corresponding ion energy of only 2.5 eV, even though we know that the IP difference is 16.1 eV. The implication seems to be that the initial cooling (say due to the first 5000 helium atoms) is extremely nonlinear with droplet size. Apparently, the first few thousand atoms are much more efficient in cooling the ions than are the rest. One possibility is that the very hot ion produced initially cools by nonthermal processes, such that the evaporation of the first few thousand helium atoms removes much more than the 5 cm^{-1}/atom expected from thermal evaporation. This seems reasonable, given that the early stages of the cooling process will be rather violent, with a very hot ion being immersed in a very cold liquid. One can certainly imagine that the helium atoms emerging from this "explosive" environment would have quite high energies and carry away a considerable amount of energy. The results in Figure 12 suggest that the first 5000 helium atoms remove approximately 13.7 eV from the molecular ion, corresponding to roughly 22 cm^{-1} per atom. This value seems reasonable in light of the results from measurements of the kinetic energy release associated with cluster ions of neon (20 cm^{-1}),[53] argon (40 cm^{-1}),[54] and krypton (40 cm^{-1}).[53]

Comparing the ion internal energy scale with the mean droplet size over the range of data points probed in the HDMS experiments, we find that the cooling from 10 000 to 40 000 atoms corresponds to only 0.16 cm^{-1}/atom, much less than the thermal value of 5 cm^{-1}/atom.[16] Apparently, the full evaporation energy of the droplet is not being used in this regime. One possibility is that only a portion of the helium droplet is evaporated in the cooling process. Indeed, if the molecular ion "explosively" evaporates from the droplet (formation of a helium gas bubble around the ion, which then expands until it bursts at the surface of the droplet), one could imagine that a large fraction of the droplet remains intact, thus not contributing to the cooling of the ion. The fact that larger droplets give more cooling could then be the result of the simple fact that the ion is likely to be further from the surface in a large droplet, making the cooling more efficient.

Although the data presented here raise some interesting issues regarding the mechanisms for cooling ions in liquid helium, it is clear that further studies will be needed before these mechanisms can be definitively established. Theoretical studies of the nature of these cooling processes would also be helpful in guiding future work.

Conclusions

We have demonstrated that the helium droplets can be used to actively cool hot molecular ions that are formed within by charge transfer. In the case of TPM, the result is a substantial reduction in the fragmentation, compared to that observed in the gas phase using electron impact ionization. From comparisons between the helium droplet results and those of the TPEPICO experiments reported here, we estimate that as much as 90% of the energy released by the charge transfer process is dissipated to the helium on the time scale of fragmentation. The initial cooling seems to be particularly effective, with the first 5000 evaporated atoms removing roughly 22 cm^{-1} per atom

(53) Parajuli, R.; Matt, S.; Echt, O.; Stamatovic, A.; Scheier, P.; Mark, T. D. *Chem. Phys. Lett.* **2002**, *352*, 288−293.
(54) Woodward, C. A.; Stace, A. J. *J. Chem. Phys.* **1991**, *94*, 4234−4242.

from the ion. The helium solvent also alters the fragmentation pathways, resulting in the appearance of new daughter ions that could be indicative of differential solvation of the various ions by the helium, thus changing the energetics and rates associated with the various fragmentation channels. The fact that the fragmentation pathways are different in helium could be used as a useful structural tool, as we come to better understand these effects, an issue that will be explored further in subsequent studies.

Acknowledgment. The authors are grateful to Pfizer for support of this research. Partial support is also acknowledged from NSF (CHE-99-87740) and AFOSR.

JA030653Q